

1 **A conceptual model-based sediment connectivity assessment for patchy agricultural catchments**

2 Pedro V. G. Batista^{1*}, Peter Fiener², Simon Scheper^{1,3}, Christine Alewell¹

3 ¹Department of Environmental Sciences, Universität Basel, Bernoullistrasse 30, 4056, Basel,
4 Switzerland.

5 ²Institute for Geography, Universität Augsburg, Alter Postweg 118, 86159, Augsburg, Germany.

6 ³Dr. Simon Scheper – Research | Consulting | Teaching, Eickhorst 3, 29413 Dähre, Germany

7

8 *pedro.batista@unibas.ch

9

10 Abstract

11 The accelerated sediment supply from agricultural soils to riverine and lacustrine environments leads
12 to negative off-site consequences. In particular, the sediment connectivity from agricultural land to
13 surface waters is strongly affected by landscape patchiness and the linear structures that separate field
14 parcels (e.g. roads, tracks, hedges, and ~~grass buffer strip~~grass buffer strips). Understanding the
15 feedbacks between these structures and sediment transfer is therefore crucial for minimising off-site
16 erosion impacts. Although soil erosion models can be used to understand lateral sediment transport
17 patterns, model-based connectivity assessments are hindered by the uncertainty in model structures
18 and input data. In particular, the representation of linear landscape features in numerical soil
19 redistribution models is often compromised by the spatial resolution of the input data and the quality
20 of the process descriptions. Here we adapted the WaTEM/SEDEM model using high resolution spatial
21 data (2 m x 2 m) to analyse the sediment connectivity in a very patchy mesoscale catchment (73 km²)
22 of the Swiss Plateau. Specifically, we used a global sensitivity analysis to explore model structural
23 ~~structural~~ assumptions about how linear landscape features (dis)connect the sediment cascade, which
24 allowed us to investigate the uncertainty in the model structure. Furthermore, we compared model
25 simulations of hillslope sediment yields from five sub-catchments to tributary sediment loads, which
26 were calculated with long-term water discharge and suspended sediment measurements. ~~Our results~~
27 ~~showed that roads were the main regulators of sediment connectivity in the catchment. In particular,~~
28 ~~the~~The sensitivity analysis revealed that the assumptions about how the road network (dis)connects the
29 sediment transfer from ~~field blocks~~field blocks to water courses had a much higher impact on
30 modelled sediment yields than the uncertainty in model parameters. ~~Moreover,~~ model simulations
31 showed a higher agreement with tributary sediment loads when the road network was assumed to
32 directly connect sediments from hillslopes to water courses. Our results ultimately illustrate how a
33 high-density road network combined with an effective drainage system increases sediment
34 connectivity from hillslopes to surface waters in agricultural landscapes ~~in this representative~~
35 ~~catchment of the Swiss Plateau~~. This further highlights the importance of considering linear landscape
36 ~~structures~~ features and model structural uncertainty in soil erosion and sediment connectivity
37 ~~models~~ research.

38

39 1 Introduction

40 Rainfall events on sloped surfaces continuously displace ~~small amounts of~~ soil particles, which are
41 transported downslope as sediments. These sediments are then stored and remobilised several times
42 before conceivably reaching surface waters. Accordingly, the sediment cascade is a natural and
43 potentially long geomorphological process (Fryirs, 2013). However, the accelerated sediment supply
44 from agricultural soils to riverine and lacustrine environments leads to negative off-site consequences.
45 Specifically, nutrient-rich and pollutant-bound particulate matter from arable land is associated to the
46 eutrophication and contamination of water courses (Krasa et al., 2019; Lacey et al., 2021). Extreme
47 erosion events in agricultural fields are also linked to the occurrence of muddy floods (Boardman,
48 2020) and to damages to downstream infra-structure (Bauer et al., 2019). Therefore, understanding
49 how and when sediment is transferred from agricultural fields to different landscape compartments is
50 imperative to reduce off-site erosion impacts.

51 The degree with which a system facilitates sediment transfer within its internal compartments is
52 defined by Heckmann et al. (2018) as sediment connectivity. This concept can be further distinguished
53 into a structural component, associated to the semi-static spatial configuration of the landscape; and a
54 functional one, which emerges as a dynamic property of the hydro-sedimentological system
55 (Wainwright et al., 2011). Connectivity theory therefore provides a framework to rethink the sediment
56 delivery problem (Fryirs, 2013; Parsons et al., 2009) and to understand the complex spatio-temporal
57 processes that regulate sediment transport.

58 In agricultural landscapes, sediment connectivity is strongly affected by the patchiness of the land use
59 configuration, and the presence of linear features between field parcels (e.g. hedges, ~~grass buffer~~
60 ~~strip~~grass buffer strips, and roads) (Alder et al., 2015; Bakker et al., 2008; Chartin et al., 2013; Fiener
61 et al., 2011; Remund et al., 2021; Van Oost et al., 2000). The importance of landscape patchiness in
62 regulating sediment transfer is specifically relevant in areas where a large number of small fields,
63 separated by linear structures, create a complex hydrological system. However, the experimental
64 analysis of sediment connectivity at catchment scale is challenging, as it involves measuring both
65 internal soil redistribution processes and cascading sediment transport rates. The interaction between
66 landscape patchiness, linear structures, and sediment connectivity is therefore not addressed by the
67 typical setup of experimental erosion studies, which either focus on small erosion plots or catchment
68 sediment yields (Fiener et al., 2019).

69 Due to the difficulties in measuring the processes that affect sediment movement at catchment and
70 landscape scale, it is common practice to analyse connectivity with modelling approaches (Nunes et
71 al., 2018). These usually rely on high-resolution process-based models, assuming they are able to
72 ~~explicitly take represent~~ connectivity ~~into account~~dynamics (Baartman et al., 2020); semi-qualitative
73 indices (Borselli et al., 2008; Cavalli et al., 2013); or more recently, the coupling of conceptual models
74 with probability theory (Mahoney et al., 2020a, 2020b). In specific, the use of process-based soil

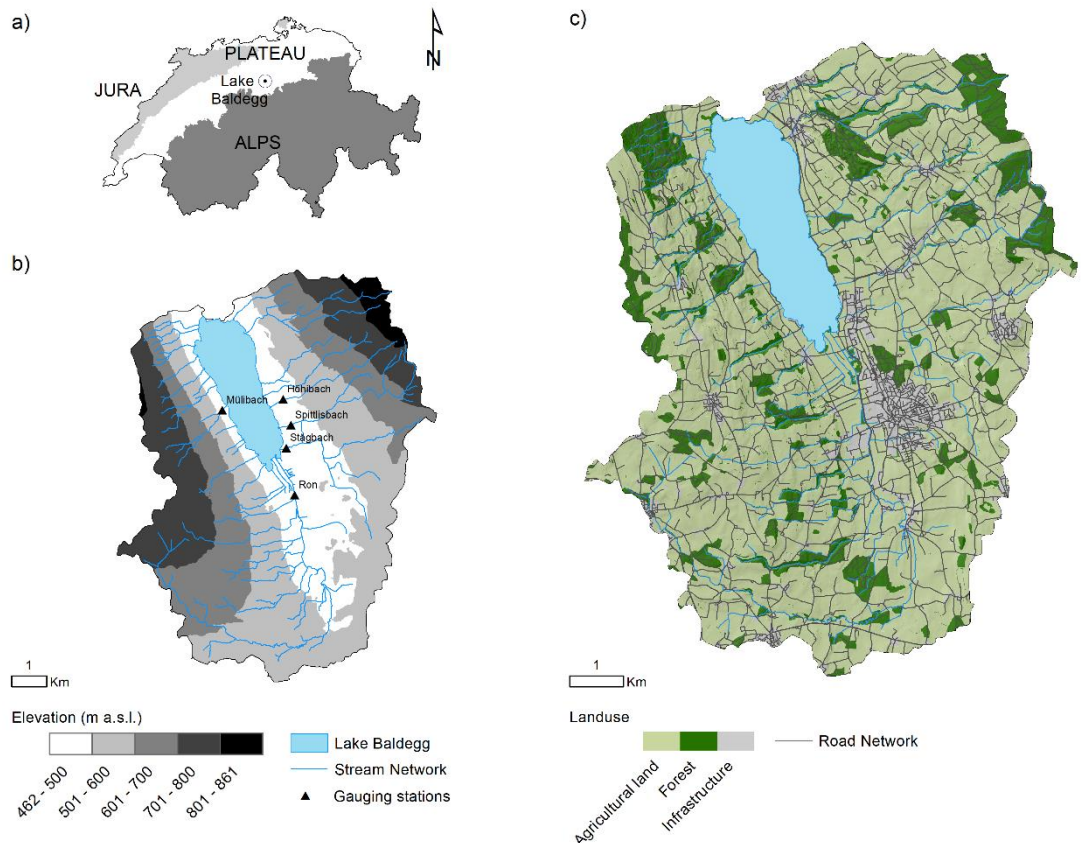
75 erosion and sediment transport models might be an important pathway to improve our understanding
76 of sediment connectivity (Nunes et al., 2018). However, erosion models in general, and process-based
77 models in particular, face two fundamental problems for representing sediment connectivity : (i) the
78 input data requirements are large and uncertain, and model application is often restricted to small
79 catchments with a maximum size of a few square kilometres (e.g. Baartman et al., 2020; Starkloff and
80 Stolte, 2014; Wilken et al., 2017) and (ii) the implemented process descriptions, especially along
81 linear landscape features and field boundaries, are weakly defined due to the aforementioned
82 unavailability of experimental data. ~~On the other hand,~~ Borrelli et al. (2018) demonstrated how parcel-
83 specific high resolution land cover and management data can improve soil erosion/sediment delivery
84 models in patchy agricultural catchments.

85 Here, we aimed to (i) adapt a conceptual soil erosion and sediment delivery model with high spatial
86 resolution data (2 m x 2 m) within a Monte Carlo framework; (ii) to analyse the sediment connectivity
87 in a very patchy mesoscale catchment (73 km²) in Switzerland; and (iii) to perform a sensitivity
88 analysis of model parameters and structural assumptions regarding how linear features (dis)connect
89 the sediment cascade. Hence, we demonstrate how models can be used to understand the interaction
90 between linear features, landscape patchiness, and sediment connectivity. This will contribute to
91 increase our comprehension of relevant connectivity processes and our ability to develop appropriate
92 measures for reducing off-site erosion impacts.

93 **2 Materials and methods**

94 **2.1 Study catchment**

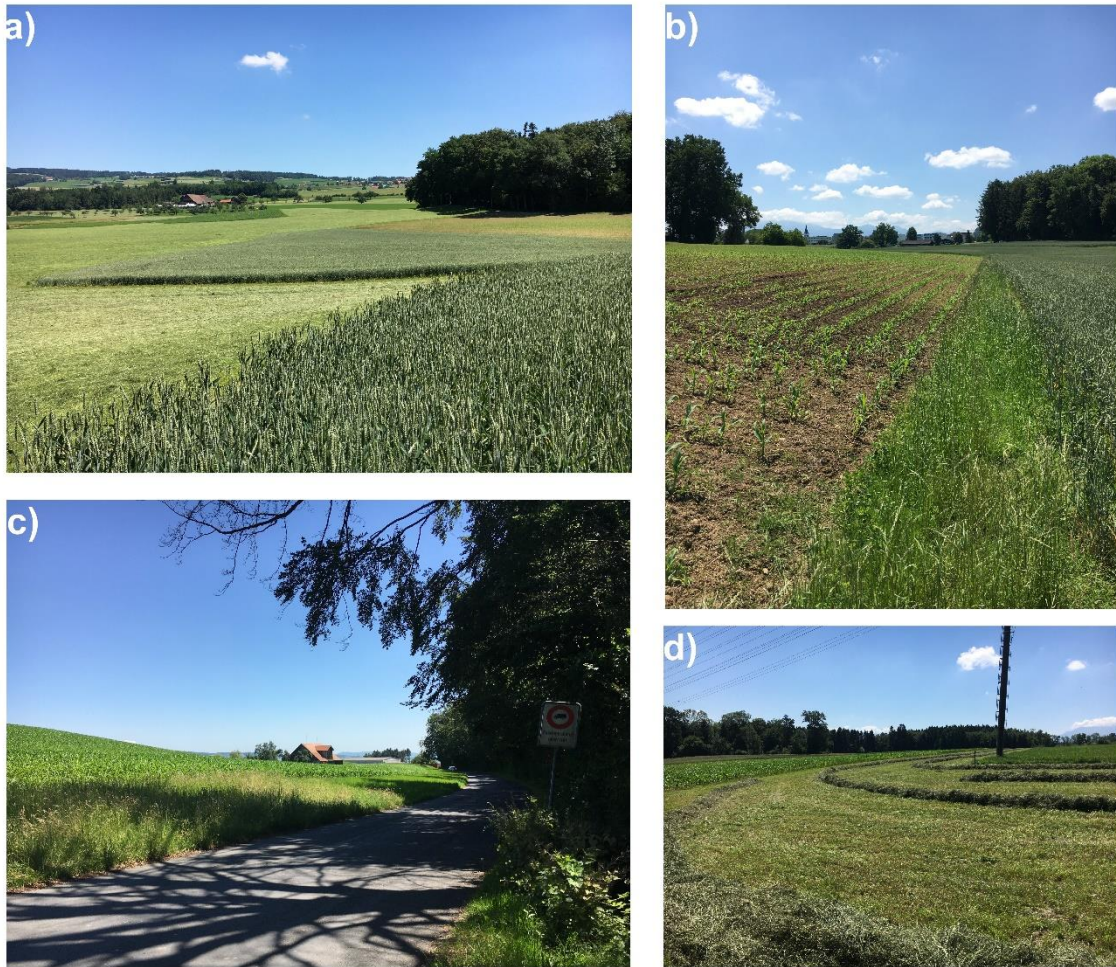
95 The study catchment consists of the contributing area of the ~~Baldeg~~-Lake Baldeg, in the central
96 Swiss Plateau (Figure 1). The lake has been extensively studied due to its hypertrophic waters, which
97 have been artificially oxygenated since 1983 (e.g. Lavrieux et al., 2019; Müller et al., 2014; Teranes
98 and Bernasconi, 2005). The eutrophication of the lake has been mostly linked to excessive phosphorus
99 loads during the 20th century (Wehrli et al., 1997). Although water quality in the lake is currently
100 improving (BAFU, 2016), the supply of phosphorus-rich sediment is still a concern to local authorities
101 (von Arb et al., 2021; Stoll et al., 2019). The major advantage of the Baldeg catchment for this study
102 is that a comprehensive hydrological data set is available based on an ongoing, long-term monitoring
103 Hence, we chose to focus our study on the Baldeg catchment by reason of the ongoing research in the
104 area and the availability of comprehensive hydrological data, which has been monitored by the
105 Department of Eenvironment and Energy of the Canton of LuzernLucerne. ~~Importantly, the~~
106 ~~catchment is representative of the patchy agricultural landscape of the Swiss Plateau, as we detail~~
107 ~~below.~~



108

109 Figure 1. a) Location of the ~~Lake~~-Baldegg catchment; b) elevation, stream network, and location of
 110 hydrological gauging stations; c) land use. Data source: Swisstopo, 2020. Sub-catchment areas:
 111 Höhibach (2.3 km²), Mülibach (1.6 km²), Stägibach (9.3 km²), Spittlisbach (3.8 km²), Ron (27.7 km²).

112 The Baldegg catchment has a total area of 73.2 km², of which 5.2 km² are covered by the lake. The
 113 remaining area is occupied by agricultural land (74%), forests (16%), and ~~settlements~~-infrastructure
 114 (e.g. settlements, developed areas, and roads) (10%) (Swisstopo, 2020) (Figure 1c). The agriculture
 115 consists of intensively managed ~~temporary~~-pastures and/or meadows, cereal production under crop
 116 rotation, permanent grasslands, fruit orchards, and small vineyards (Lavrieux et al., 2019; Stoll et al.,
 117 2019). The majority of the meadows are composed of a mixture of grasses and clover, which are
 118 harvested for silage, hay, or barn feeding up to six times per year (von Arb et al., 2021). Agricultural
 119 ~~field blocks~~field blocks, here delimited by external boundaries (e.g. roads, water courses, and forests)
 120 (Bircher et al., 2019), have a median size of 4.4 ha. However, smaller patches separated by hedges,
 121 tree lines, and ~~grass buffer strip~~grass buffer strips, are generally found within the blocks (Figure 2).



122

123 Figure 2. Typical agricultural landscapes from the Baldegg catchment: a) Small arable and grassland
 124 patches within larger ~~field blocks~~ field blocks, b) ~~Grass buffer strip~~ Grass buffer strip between maize
 125 and wheat fields, c) wide ~~grass buffer strip~~ grass buffer strip between maize field and a vicinal road, d)
 126 freshly cut hay from a pasture in between maize fields.

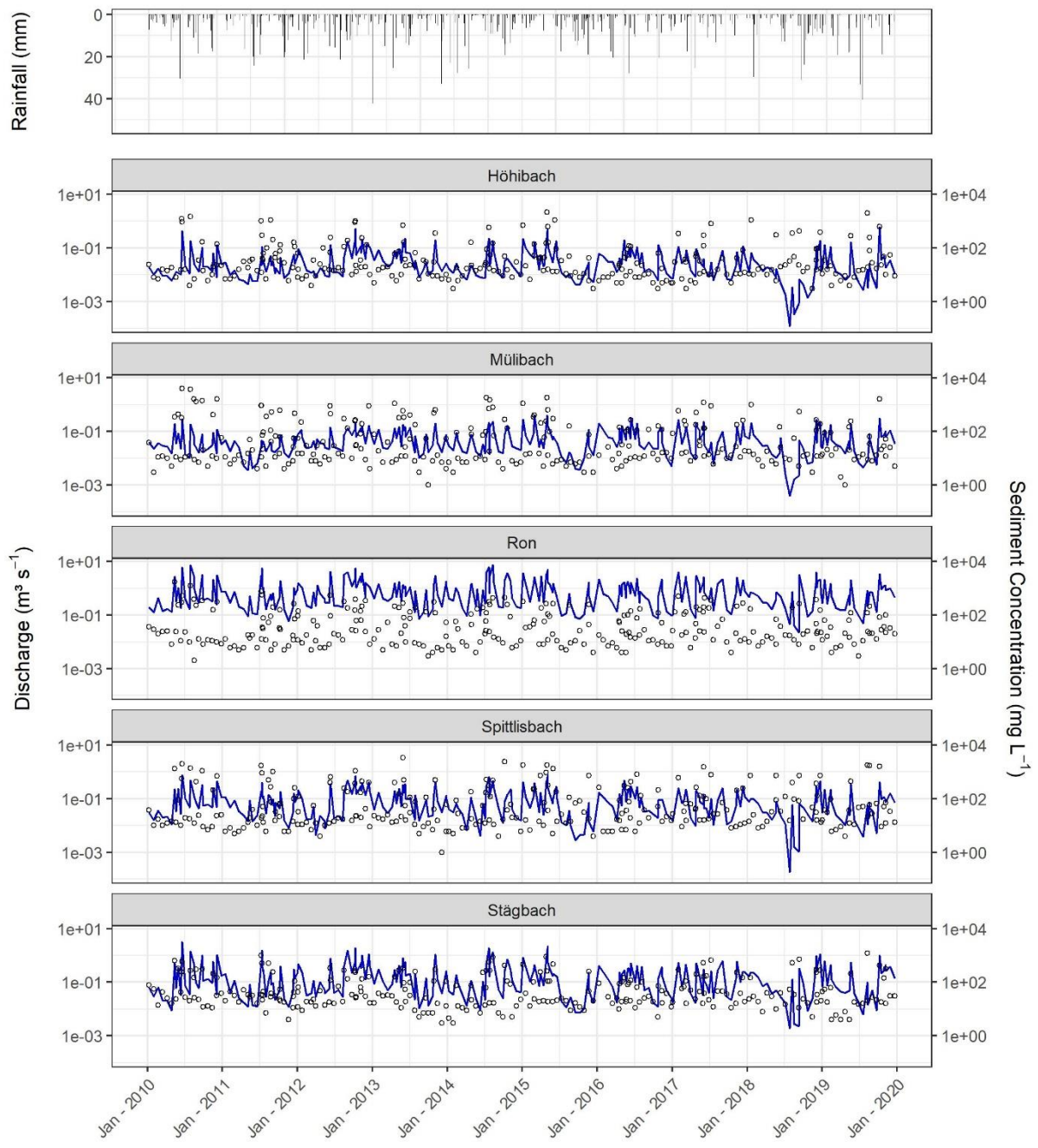
127 The road network density in the Baldegg catchment is 6.0 km km^{-2} , which is approximately three
 128 times higher than the stream density (1.9 km km^{-2}). Streams in the upper catchment are often incised,
 129 with visible, yet not prominent, signs of bank erosion. ~~Flow is sometimes regulated in the lowland~~
 130 ~~areas, and tile drainage is found at water accumulation zones (Stoll et al., 2019).~~ A total of 22 channels
 131 flow into the Baldegg-Lake Baldegg, of which five streams are monitored for water and sediment
 132 discharge by cantonal authorities, as described in section 2.2.

133 ~~The E~~elevation in the Baldegg catchment ranges from 462 to 861 m ~~a.s.l.~~ Steeper slopes (~~maximum~~
 134 ~~above 1035°~~) and higher altitudes are found in the eastern and western sides of the catchment (Figure
 135 1b), in a typical glacial landscape of the Swiss Plateau – in this case formed by the retreat of the Reuss
 136 Glacier in the south to north direction (~18,000 years BP) (Keller, 2021; Pfiffner, 2021). As a result,

137 calcaric Cambisols ([IUSS Working Group WRB, 2006](#)) developed upon Tertiary and Quaternary
138 deposits are the main soil class in the catchment. Rainfall is well distributed throughout the year,
139 although greater precipitation is observed from May to August. The average annual rainfall (2010-
140 ~~2020~~2019) at the closest gauging station is $\sim 1000 \text{ mm yr}^{-1}$ (Mosen, 454 m a.s.l., $\sim 3.5 \text{ km}$ north of the
141 ~~Baldegg-Lake lake~~Baldegg, acquired from MeteoSwiss 2021) and mean rainfall erosivity in the
142 catchment is $\sim 1150 \text{ MJ mm ha}^{-1} \text{ h}^{-1} \text{ yr}^{-1}$ (Schmidt et al., 2016).

143 2.2 Tributary suspended sediment loads

144 Suspended sediment concentrations from five tributaries ~~flowing into to~~ the Baldegg-Lake Baldegg
145 ~~were are measured monitored during ten years (Jan 2010—Dec 2019)~~ by the Department of
146 Environment and Energy of ~~the Canton of Luzern~~Lucerne. ~~Here, we used the data measured from Jan~~
147 ~~2010 to Dec 2019. Approximately~~ On average 2745 grab samples were taken from each tributary,
148 which corresponds ~~roughly to two one~~ samples every 22 days, ~~per month, and plus additional samples~~
149 ~~collected during~~ high-flow events (10 – 13 per year) ~~were opportunistically sampled~~ (Figure 3).
150 Suspended sediments were measured at the same location where water discharge was monitored by
151 automatic gauging stations (Figure 1b). A summary of the measured rainfall, water discharge, and
152 sediment concentration from 2010 to ~~2020-2019~~ is displayed in Figure 3.



153

154 Figure 3. Daily rainfall at the Mosen station, mean daily discharge (blue line), and sediment
 155 concentration (circles) at the monitored tributaries of the ~~Baldegg Lake~~ Lake Baldegg (2010-2019).
 156 Data source: MeteoSwiss (2021).

157 In order to calculate the sediment load for the monitored tributaries, we fitted a rating curve (Equation
 158 1) with the measured sediment concentrations and their correspondent ~~water—discharge~~
 159 ~~values~~discharge. Additional covariates were included to account for hysteresis, seasonality, and
 160 constituent exhaustion (Table 1) (Vigiak and Bende-Michl, 2013; Wang et al., 2011):

$$\ln c_i = \beta_0 + \sum_{k=1}^5 \beta_k x_{k,i} + \varepsilon_i \quad (1)$$

161

162 Where: c is sediment concentration (mg L^{-1}) for day i , β_0 is the intercept, β_k are fitted coefficients, x_k
 163 are covariates (Tab. 1) accounting for discharge, hysteresis, seasonality and constituent exhaustion, k
 164 is the covariate identification, and ε_i is the residual error.

165 Table 1. Covariates used for fitting the sediment-rating curve, as in Vigiak and Bende-Michl (2013)
 166 and Wang et al. (2011).

Covariate	Expression	Explanation	Physical interpretation
$x_{1,k}$	$\ln Q_i$	Q_i is water -discharge for day i (m^3s^{-1})	Discharge
$x_{2,k}$	$(\ln Q_i)^2$	Quadratic term of $x_{1,i}$ Q_i	Hysteresis
$x_{3,k}$	$\sin(2\pi M_i/12)$	M_i = month of day i	Seasonality
$x_{4,k}$	$\cos(2\pi M_i/12)$	M_i = month of day i	Seasonality
$x_{5,k}$	$\frac{\sum_{z=1}^i 0.95^{i+1-z} Q_z}{\sum_{z=1}^i 0.95^{i+1-z}}$	Discount flow up to day i	Constituent exhaustion (see Wang et al., 2011)

167

168 The rating curve was used to estimate daily sediment concentrations for the entire 2010-~~2020-2019~~
 169 period. Subsequently, we propagated the uncertainty in the regression fit by simulating posterior
 170 distributions of the model coefficients (β_0 , β_k) with an informal Bayesian function of the R package
 171 ‘arm’ (Gelman and Hill, 2007), as in Batista et al. (2021). The posterior distributions were used to
 172 simulate 1000 sediment concentration values for each day i . These were transformed into daily
 173 distributions of sediment loads (Mg), considering the mean daily discharge measurements from the
 174 gauging stations. Sediment loads were ultimately aggregated into average annual values (Mg yr^{-1}).

175 2.3 Model description

176 A modified version of the spatially distributed erosion and sediment transport WaTEM/SEDEM (Van
 177 Oost et al., 2000; Van Rompaey et al., 2001; Verstraeten et al., 2010) was used in this study.
 178 WaTEM/SEDEM provides a framework for modelling sediment connectivity from hillslope to water
 179 courses by use of a steady_-state transport capacity equation and a pixel-based sediment routing

180 component. That is, the model assumes that soil particles displaced by water erosion at a given grid-
 181 cell are transferred downstream for as long as the runoff transport capacity is greater than the sediment
 182 supply, or until the flow path reaches a definite sink. Although the model is able to simulate both
 183 tillage and water erosion, here we focus on the latter, which is calculated with an adaptation of the
 184 RUSLE (Renard et al., 1997) (Equation 2). We chose to focus on soil erosion by water because in
 185 WaTEM/SEDEM the sediment supply/routing is not affected by tillage erosion. However, tillage
 186 erosion is likely to be an important within-field soil redistribution process in the catchment (please see-
 187 as we will explain in the discussion below). The model is by default executed in an average yearly
 188 time step, as is typical in RUSLE applications:

$$A = R K LS_{2d} C P \quad (2)$$

190

191 Where: A is average annual soil loss ($\text{kg m}^{-2} \text{yr}^{-1}$), R is rainfall erosivity ($\text{MJ mm m}^{-2} \text{h}^{-1} \text{yr}^{-1}$), K is soil
 192 erodibility ($\text{kg h MJ}^{-1} \text{mm}^{-1}$), LS_{2d} is a topographic factor calculated by the Desmet and Govers (1996)
 193 procedure (dimensionless), C is a cover-management factor (dimensionless), and P is a support
 194 practice factor (dimensionless).

195 Transport capacity ($\text{kg m}^{-1} \text{yr}^{-1}$) per unit widths of grid cells is assumed to be proportional to the
 196 potential to rill erosion, which is described by a power function of slope length and gradient (Van
 197 Rompaey et al., 2001):

198

$$TC = K_{TC} R K (LS_{2d} - 4.12 S_g^{0.8}) \quad (3)$$

199

200 Where: K_{TC} is a landuse-dependent transport capacity coefficient (m) which requires calibration, R is
 201 rainfall erosivity ($\text{MJ mm h}^{-1} \text{yr}^{-1}$), K is soil erodibility ($\text{t h MJ}^{-1} \text{mm}^{-1}$), LS_{2d} is a topographic factor
 202 calculated by the Desmet and Govers (1996) procedure (dimensionless), and S_g is slope gradient (m m^{-1}).
 203

204 WaTEM/SEDEM partially incorporates the influence of the landscape structure on sediment transfer
 205 by the use of a parcel connectivity parameter P_{Con} , which represents the proportion of sediment that is
 206 stopped at field borders. The model also simulates runoff connectivity by means of a parcel trapping
 207 efficiency P_{TEf} parameter, which corresponds to the proportion of the flow accumulation that is routed
 208 downstream. Finally, the model is able to estimate the total amount of sediment transferred from
 209 hillslopes to water courses, which can be interpreted as the hillslope component of a catchment
 210 sediment budget. Since WaTEM/SEDEM does not represent gully and bank, channel-erosion, nor in-
 211 stream erosion and deposition processes, any comparison between modelled sediment yields and

212 catchment-outlet sediment loads must be interpreted with ~~upmost~~ caution. However, in catchments
213 where rill and interrill are the main overland erosion processes, and assuming a state of long term
214 fluvial quasi equilibrium, the outlet sediment loads should be at least comparable to the model outputs
215 – even if not fully commensurable. For further information on the model, we refer to Notebaert et al.,
216 (2006), Van Oost et al., (2000), Van Rompaey et al., (2001), and Verstraeten et al., (2010).

217 **2.4 Model implementation, input data, and sensitivity analysis**

218 WaTEM/SEDEM is ~~usually~~ implemented ~~with as~~ a user-friendly GUI developed at KU Leuven
219 ~~(Notebaert et al., 2006), and freely available at~~
220 ~~<https://ees.kuleuven.be/geography/modelling/watemsedem/>.~~ Although the software facilitates model
221 application, it does not allow for more complex operations, such as sensitivity or uncertainty analysis.
222 Moreover, some model components might not be fully comprehensible without access to the source-
223 code, and WaTEM/SEDEM is frequently used as a black-box. Hence, in order to perform a sensitivity
224 analysis of model parameters and underlying structural model assumptions, we implemented a
225 WaTEM/SEDEM version using the free open source software R (R Core Team, 2021) and SAGA GIS
226 (Conrad et al., 2015). The main adaptations are described in the following, and our code is available as
227 supplementary material.

228 Our model application consists of a global all-at-a-time sensitivity analysis, as described by Pianosi et
229 al. (2016). That is, we performed a Monte Carlo simulation to explore the variability of the whole
230 parameter space, and all input factors were sampled simultaneously for each model realisation ($n =$
231 1200). The framework is similar to an uncertainty analysis, except in this case we did not focus on
232 ~~quantifying uncertainty or~~ locating the parameter space which produced behavioural model
233 realisations. Instead, we concentrated on apportioning sources of uncertainty to different model input
234 factors, aiming to rank their contribution to the variability of the response surface (see Pianosi et al.,
235 2016 for a review on sensitivity analysis). This should allow us to identify parameters and model
236 assumptions that have a greater impact on the manner with which WaTEM/SEDEM describes
237 sediment connectivity in the Baldegg catchment. In particular, the analysis of different assumptions
238 about the structure of the model should provide a connectivity assessment based on the quantification
239 of the structural uncertainty within the simulations. To the best of our knowledge, this is the first time
240 the analysis of model structural error is incorporated to sediment connectivity research.

241 For each iteration of the Monte Carlo simulation, all RUSLE input variables were sampled from
242 uniform distributions, except for the LS_{2d} factor (Table 2). Minimum and maximum R factor values
243 were retrieved from the Swiss national map (Schmidt et al., 2016), and a single lumped value for the
244 whole catchment was sampled for each iteration. The same approach was used for the K factor
245 (Schmidt et al., 2018a). We used lumped catchment values for these factors due to their low spatial
246 variability within the study area, according to the national maps (coefficient of variations are 1% and
247 7% for the K and R factor, respectively). For the C and P factors, here combined in a single CP

248 parameter, uniform distributions were created for each landuse class in the catchment, based on
249 commonly used values from the literature and a ~~rasterised (2 m x 2 m)~~ land cover map (1:25000)
250 (Swisstopo, 2020), which we rasterised to the model resolution (2 m x 2 m). Due to the unavailability
251 of open source geodata of spatially distributed crop statistics in the Baldegg catchment, pastures and
252 cropland were aggregated into a single arable land category (Table 23). In this case, minimum and
253 maximum values were relaxed to represent a wide possible combination of crops and support
254 practices. Such combinations were assessed with the *CP*-Tool (Kupferschmied, 2019), which allows
255 for the calculation of *CP* values considering common crop rotation systems in Switzerland. The
256 minimum *CP* values were particularly reduced to include typical values for permanent grasslands in
257 Switzerland (~0.01) (Schmidt et al., 2018b). Finally, the LS_{2d} factor was calculated with a slope (rad)
258 and an upslope contributing area (m^2) grid, which were obtained by processing a 2 m x 2 m resolution
259 DEM from SwissALTI3D (Swisstopo, 2014a).

260 Table 2. Minimum and maximum parameter values sampled during the Monte Carlo simulation.

Parameter	Category	Min	Max
R (MJ mm m ⁻² h ⁻¹ yr ⁻¹)		950 10 ⁻⁴	1350 10 ⁻⁴
K (kg h MJ ⁻¹ mm ⁻¹)		0.025 10 ³	0.040 10 ³
CP (-)	Arable land	0.01	0.5
	Grass buffer strip Grass buffer strips	0.001	0.009
	Forest	0.0001	0.003
	Orchard	0.001	0.2
	Vineyard	0.05	0.6
K_{TC} (m)	High (arable land, vineyard)	1	200
	Low (grass buffer strips, forest, orchard)	1	100
P_{TEf} (-)		0	1
P_{Con} (-)		0	1

261

262 Similarly, all WaTEM/SEDEM-specific model parameters were sampled from uniform distributions
 263 (Table 2). Landuse classes with a CP factor above 0.01 received higher transport capacity coefficients
 264 (K_{TC} high). The remaining landuse classes, namely forests and grass strips, received lower coefficients
 265 (K_{TC} low). The K_{TC} reference values were taken from Van Rompaey et al. (2001) and extended in order
 266 to explore a larger parameter space. The sampled parcel trapping efficiency (P_{TEf}) values were
 267 assigned to forests and ~~grass buffer strip~~ grass buffer strips in the rasterised land cover map, as we
 268 explain below. The resulting P_{TEf} grid was used as a weight for calculating the aforementioned upslope
 269 contributing area. Hence, only a proportion of the grid-cell area from forests and grass strips
 270 contributed to the downstream flow accumulation, as runoff amounts are assumed not to increase (or
 271 to increase slowly) with slope length under natural vegetation (Govers, 2011). Parcel connectivity
 272 (P_{Con}) values were assigned to the forest and ~~grass buffer strip~~ grass buffer strips cells that bordered
 273 agricultural fields, representing the extent with which water and sediment transport is reduced at parcel
 274 borders (Notebaert et al., 2006). The transport capacity (Eq. 2) at these cells was reduced by a fraction
 275 inversely proportional to the sampled P_{Con} value.

276 For each sampled combination of parameters values, the models were ran with and without the
 277 presence of ~~grass buffer strip~~ grass buffer strips between agricultural ~~field blocks~~ field blocks and
 278 adjacent roads and forests. Although ~~grass buffer strip~~ grass buffer strips are generally present at field
 279 borders in the Baldegg catchment (Figure 2), these features were not distinguishable in the land cover
 280 map. Hence, we manually inserted 2 m wide ~~grass buffer strip~~ grass buffer strips at the aforementioned
 281 borders. The extent of the buffer-strips in reality is quite variable, and generally wider at forest and
 282 river vicinities (3 – 6 m), as required by law in Switzerland (Alder et al., 2015). For simplicity, we
 283 used a single value that should allow us to test the sensitivity of the model to the presence of the strips.
 284 The 2 m width was selected based on the spatial resolution of the model input data. On the other hand,
 285 hedges and tree lines within ~~field blocks~~ field blocks were already classified in the land cover map, and
 286 required no additional processing.

287 Furthermore, three road connectivity assumptions were assessed for each model iteration. In a first
288 scenario, roads were treated as an ultimate sink, with zero transport capacity (i.e. ‘roads as sinks’).
289 Hence, sediments reaching roads or infrastructure were subsequently removed from the system and did
290 not reach surface waters. This represents a scenario in which ~~road and field drainage~~ roadside ditches
291 and the road drainage system -traps most sediments and partly diverges runoff to wastewater treatment
292 plants. A second scenario assumed that all sediments reaching the road network were directly
293 connected to the stream network. This represents a situation in which the road drainage system acts as
294 a hydrological-hydraulic shortcut, transferring sediments from fields into surface waters (i.e. ‘roads as
295 shortcuts’) (see Schönenberger and Stamm, 2021). As in the original model formulations (see
296 Notebaert et al., 2006), the third scenario assigned very high transport capacity to roads and
297 infrastructure, so that no deposition would take place (i.e. ‘roads as patch_-connectors’). In this case,
298 runoff and sediment might flow along or across the road network – which is expected to happen
299 during extreme rainfall events when the drainage system is clogged. For this scenario, deposition will
300 never occur on road cells, however sediments can still be deposited on lower patches, before reaching
301 the stream network. Hence, sediment transfer will be entirely dependent on the flow direction
302 calculated from the DEM. Here we employed a multiple flow direction algorithm, which was used for
303 calculating upslope contributing area and routing sediments along the flow p-path. The sediment
304 routing component was implemented with a capacity accumulation function from SAGA GIS (Conrad
305 et al., 2015), ~~and~~. ~~Of note~~, all geo-processing tools were applied with the ‘RSAGA’ package
306 (Brenning et al., 2018). ~~Additional R packages essential to the simulations were ‘doParallel’ (Ooi et~~
307 ~~al., 2019), ‘foreach’ (Calway and Weston, 2017), ‘raster’ (Hijmans, 2020), and ‘rgdal’ (Bivand et al.,~~
308 ~~2019).~~

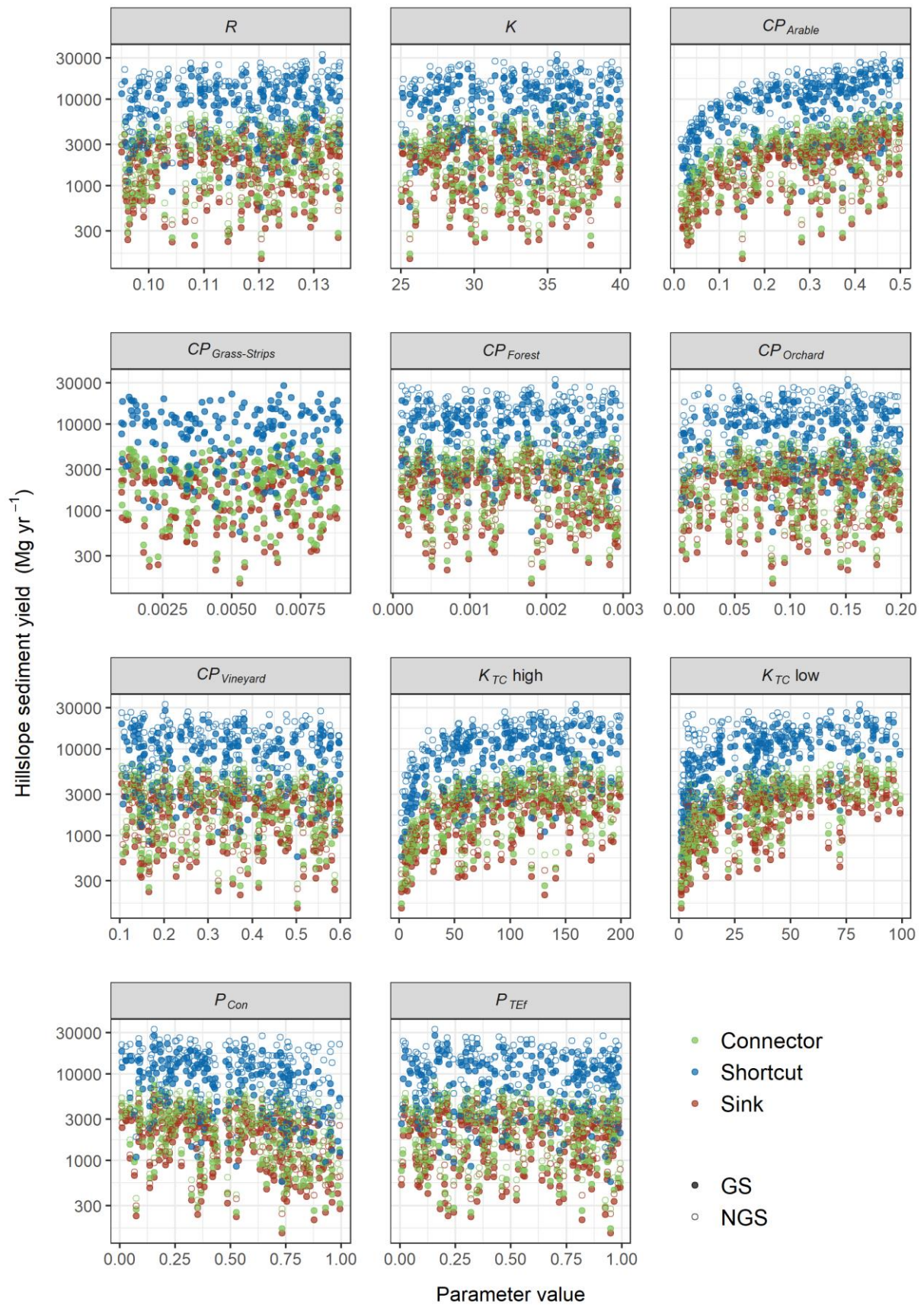
309 The sensitivity of WaTEM/SEDEM to the uncertainty in model parameters, the presence of ~~grass-~~
310 ~~buffer strip~~ grass buffer strips, and assumptions about road connectivity (i.e., model structural
311 uncertainty) was assessed by evaluating modelled hillslope sediment yields (i.e., the amount of
312 sediment delivered from hillslopes to surface waters) for the entire Baldegg catchment. A qualitative
313 analysis was performed with a visual inspection of scatter plots, comparing the univariate parameter
314 space with the model response surface. Additionally, we used a random forest analysis (RFA) to rank
315 the importance of input factors to the uncertainty in model outputs (Antoniadis et al., 2021). That is, a
316 random forest ~~was used to predicted~~ predict the WaTEM/SEDEM-modelled sediment yields, based on
317 the sampled parameter values ~~in for each iteration of~~ the Monte Carlo simulation. The importance of
318 the input factors, including model parameters, the presence of grass-strips, and the road connectivity
319 scenarios, was ranked based on their relative contribution to the RFA predictive error, following an
320 out-of-bag estimate (Breiman, 2001). We chose the RFA due to its ability to rank both qualitative and
321 quantitative input factors. The analysis was performed with the ‘randomForest’ (Liaw and Wiener,
322 2002) R package.

323 Finally, we compared the resulting WaTEM/SEDEM simulations of sub-catchment hillslope sediment
324 yields to the suspended sediment loads from the monitored tributaries. Of note, with this comparison
325 we only aim to provide a general picture of the plausibility of the model realisations. Suspended
326 sediment loads are a product of a complex interaction of hillslope and channel remobilisation
327 processes, which are not fully represented by WaTEM/SEDEM. Hence, modelled hillslope yields and
328 suspended loads are not fully-entirely commensurable, and we did not focus on a rejectionist
329 framework for model testing. This research is exploratory, and exploratory and investigates the
330 importance of linear features and landscape patchiness on sediment connectivity.

331 **3 Results**

332 **3.1 Sensitivity analysis**

333 The road connectivity assumptions were by far the most sensitive input factor for WaTEM/SEDEM in
334 the Baldegg catchment. This can be easily visualised is illustrated in Figure 4, which presents scatter
335 plots comparing sampled parameter values and the model response surface. The uniformly scattered
336 points denote a low sensitivity of the modelled hillslope sediment yields to most input factors, with
337 some evident exceptions: CP for arable land, K_{TC} high, and K_{TC} low. On the other hand, all plots
338 demonstrate that higher sediment yields were calculated when we assumed that roads behaved as
339 hydrological-shortcut hydraulic shortcuts, directly connecting agricultural patches to the stream_
340 network.

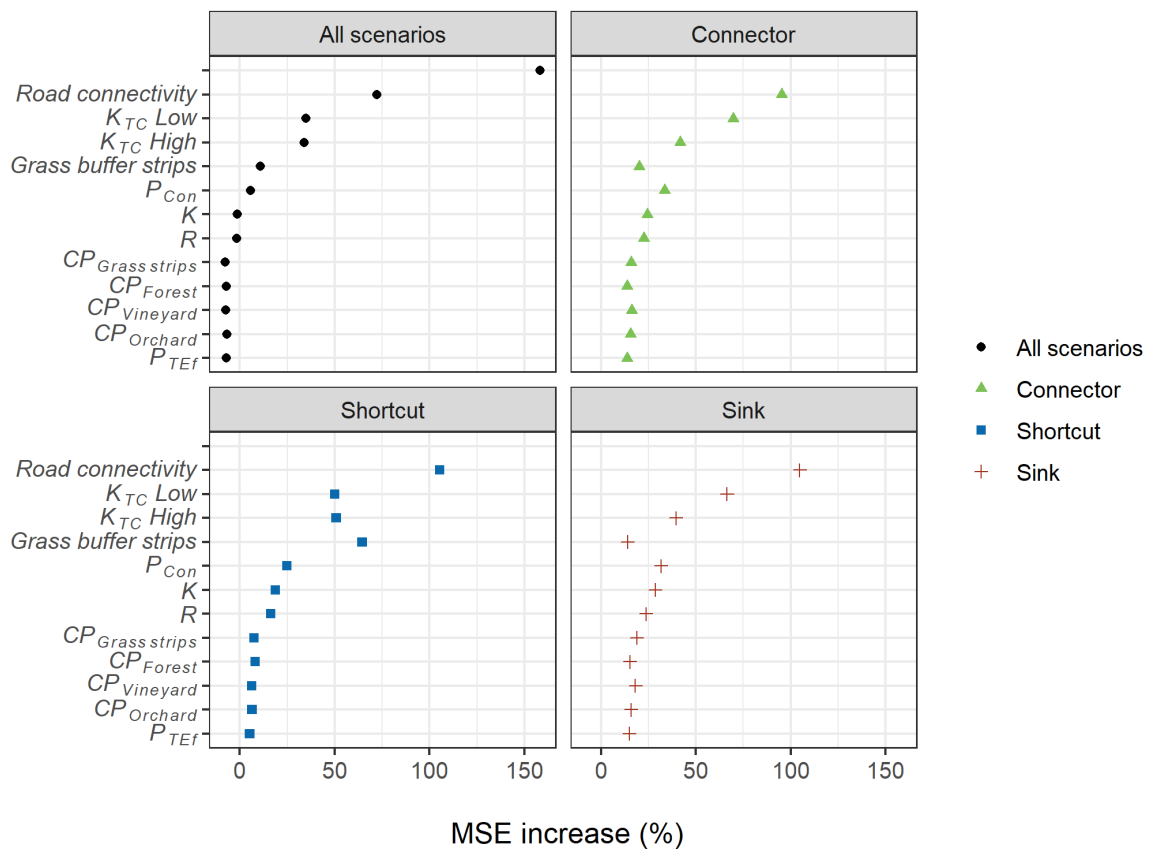


341

342 Figure 4. Univariate scatter plots of sampled parameter values. Full circles represent model
 343 realisations with the presence of ~~grass buffer strip~~ grass buffer strips (GS), and open circles represent

344 the ones without strips (NGS). Colours represent the road connectivity assumptions (i.e. 'roads as
345 patch_connectors', 'roads as ~~hydrological shortcuts~~hydraulic shortcuts', and 'roads as sinks'). See
346 section 2.4 for a description of road connectivity scenarios.

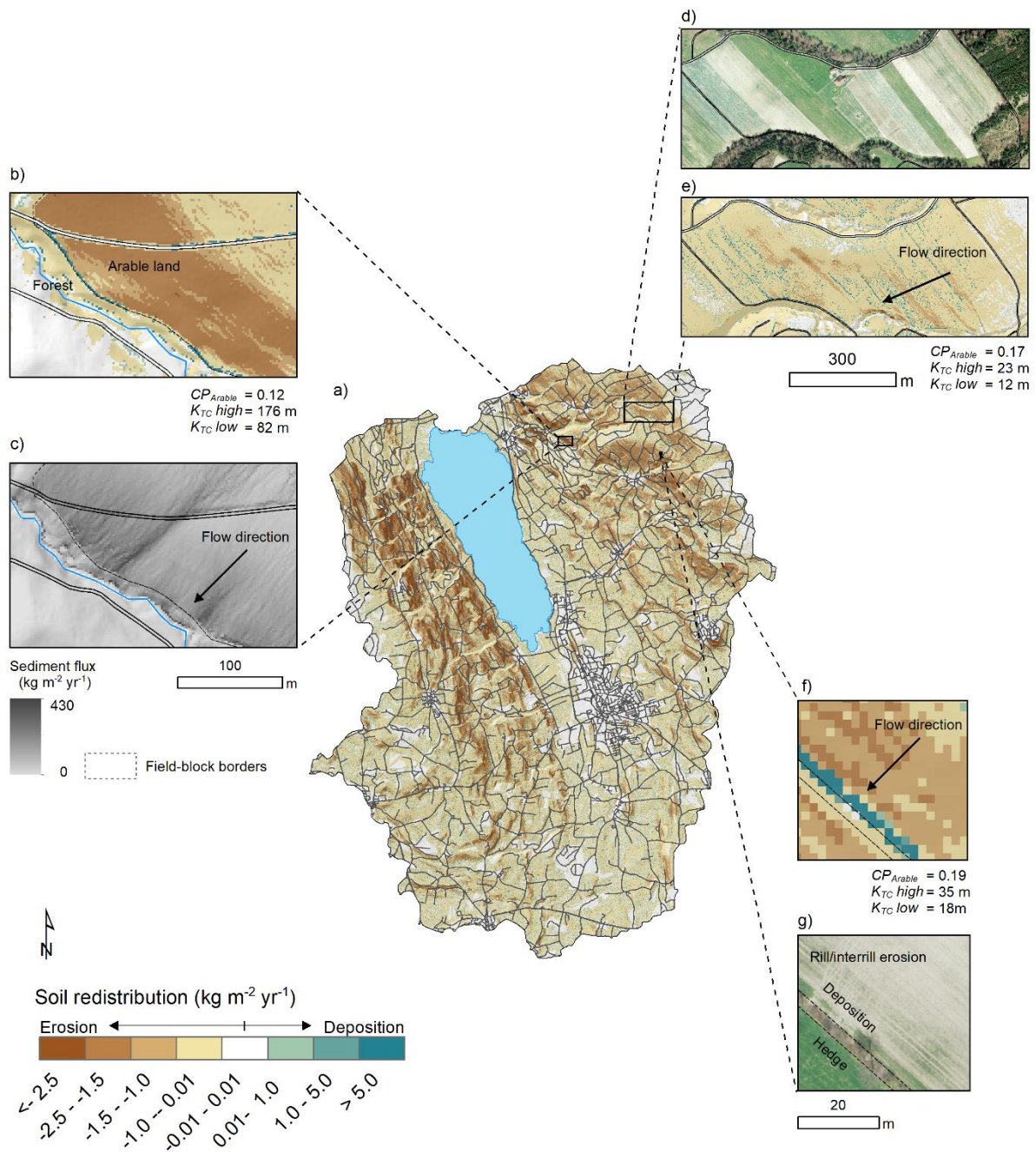
347 Similarly, the results from the RFA demonstrate that road connectivity was the most important input
 348 factor for predicting the WaTEM/SEDEM outputs (Figure 5). That is, if road connectivity was not
 349 considered, the predictive mean squared error (MSE) of the RFA increased by 175.158%. The
 350 MSE increase associated to *CP* for arable land (72%~~67.3%~~), K_{TC} low (35%~~6%~~), K_{TC} high (34%~~3%~~),
 351 and the presence of grass buffer strips (1127.0%), indicate the model was also
 352 sensitive these input factors. However, if we considered each road connectivity scenario individually,
 353 the results from the random forest were shifted, as the model seemed to be more sensitive to the
 354 presence of grass buffer strips for the ‘road as shortcuts’ scenario (MSE increase =
 355 6543.6%).



356
 357 Figure 5. Mean squared error (MSE) increase associated to model input factors for the RFA. Larger
 358 relative errors indicate the input factors were more important for estimating model outputs.

359 3.2 Spatial patterns

360 The spatial patterns of soil redistribution rates were also highly influenced by linear features,
 361 landscape patchiness, and connectivity assumptions. Sediment deposition on field blocks
 362 downslope from roads was more frequently observed for the ‘roads-as-connectors’ scenario, than for
 363 the other road connectivity assumptions. Specifically, when sediments were not diverged or trapped by
 364 the road network, there was a greater proportion of sediment deposition on foot slope field
 365 borders and other potential sinks (Figure 6b).



367

368 Figure 6. a) Catchment patterns of soil redistribution for a model ~~a~~-realisation with the presence of
 369 ~~grass buffer strip~~ grass buffer strips; b) detail of sediment deposition on field borders, ‘road as patch
 370 connectors’ scenario; c) detail of sediment fluxes across the road network, ‘road as patch connectors’
 371 scenario; d) detail of aerial image of multiple parcels within a field_block (Swisstopo, 2014b); e) soil
 372 redistribution rates for the field_block; f) detail of sediment deposition at a ~~grass buffer strip~~ grass
 373 buffer strip at a field border; g) aerial image for the field (Swisstopo, 2014b).

374

375 The sediment flux from agricultural fields was generally interrupted when entering forest patches, and
 376 further deposition was modelled at forested valley floors, near the stream channels, for all scenarios
 377 (Figure 6b, c). Importantly, sediment deposition along ~~grass buffer strip~~ grass buffer strips, hedges,
 378 and tree lines reduced sediment fluxes in between ~~field blocks~~ field blocks, forming a patchy
 379 connectivity pattern. This was again visible for all simulated connectivity assumptions, albeit
 380 particularly pronounced when the presence of ~~grass buffer strip~~ grass buffer strips was considered
 381 (Figure 6 a, f).

382 Unexpectedly, the soil redistribution patterns revealed that WaTEM/SEDEM simulated linear
 383 deposition areas at the borders of small cropland patches (Figure 6d, e). This occurred even in the
 384 absence of ~~grass buffer strip~~ grass buffer strips or hedges, and hence without P_{Con} parameterisation,
 385 which was only applied to field-block borders. These depositional patterns were particularly evident
 386 within ~~field blocks~~ field blocks oriented across the slope direction, and apparently stem from small_
 387 scale changes in the slope gradient, which were represented by the high-resolution DEM and which
 388 potentially results from long_
 389 term tillage erosion.

389 3.3 Soil redistribution rates, hillslope sediment-yields, and suspended sediment loads

390 Soil redistribution rates for eroding grid_
 391 cells in the Baldegg catchment were almost identical among
 392 the simulated road connectivity assumptions (Table 3). Higher absolute deposition rates were
 393 calculated for the simulations without grass_
 394 strips for both the connector and sink scenarios, which is
 395 a result of increased erosion rates calculated without the presence of the strips. On the other hand,
 396 lower sediment yields were calculated with the presence of ~~grass buffer strip~~ grass buffer strips when
 397 the connectivity scenarios were analysed individually. Among these scenarios, deposition rates were
 398 lower if roads were considered to behave as ~~hydrological shortcuts~~ hydraulic shortcuts. Contrarily,
 399 deposition rates for the ‘roads as connectors’ and ‘roads as sinks’ scenarios were very similar,
 400 although road deposition was only modelled in the second case. Therefore, deposition rates within
 401 fields, patch_
 402 borders, colluviums, and valley_
 403 floors for the connector scenario were ~30% higher than
 404 for the other simulations. As the sediments not diverged by the road network were ultimately
 405 deposited within the catchment, the sink and connector scenarios displayed very similar hillslope
 406 sediment yields. Contrarily, sediment yields for the shortcut scenario were in general ~4.5 times higher
 407 than for the remaining road connectivity simulations.

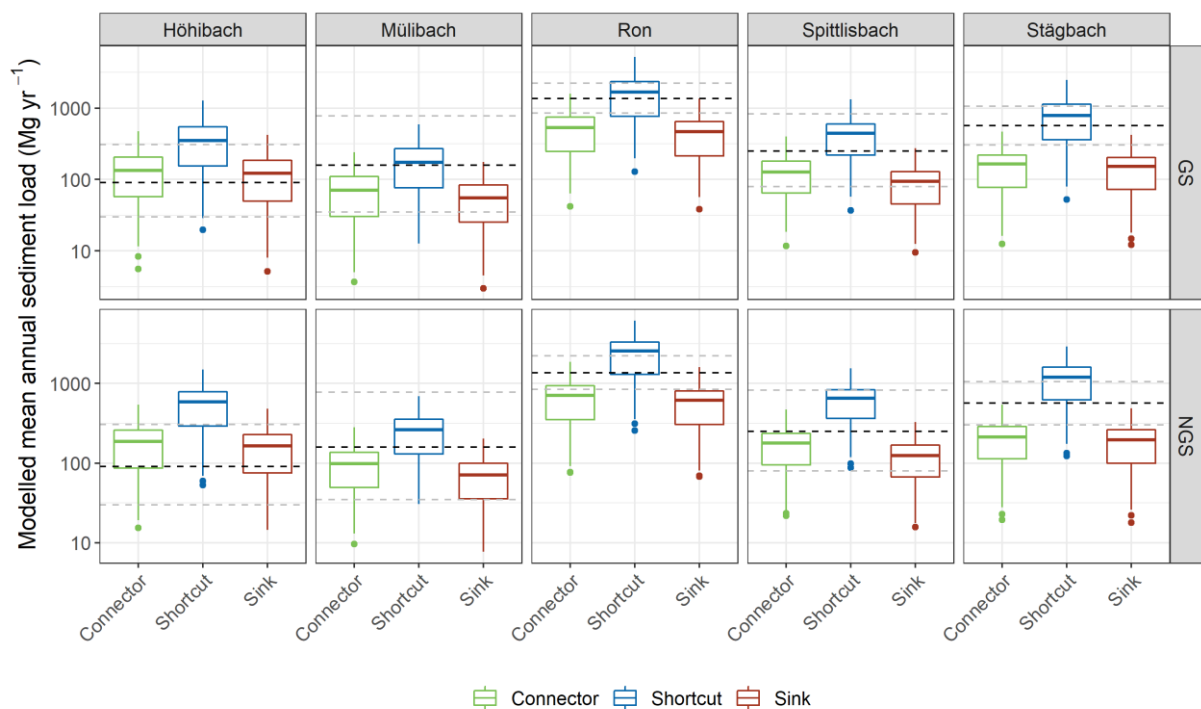
404 Table 3. Summary statistics of soil redistribution rates, hillslope sediment yields calculated by the
 405 WaTEM/SEDEM simulations.

Scenario	Erosion			Deposition			SSY			SY			
	----- Mg ha ⁻¹ yr ⁻¹ -----									----- Mg yr ⁻¹ -----			
	Q1	Q2	Q3	Q1	Q2	Q3	Q1	Q2	Q3	Q1	Q2	Q3	
Connector	GS	3.5	6.3	8.7	3.4	5.9	8.3	0.2	0.3	0.5	1,047	2,248	3,307
	NGS	3.7	6.6	9.1	3.5	6.1	8.5	0.2	0.4	0.6	1,498	3,054	4,097

Shortcut	GS	3.5	6.3	8.8	2.7	4.9	7.2	0.6	1.2	1.8	3,878	8,467	12,242
	NGS	3.7	6.6	9.2	2.5	4.7	6.7	0.9	1.9	2.6	6,303	13,238	17,506
Sink	GS	3.5	6.3	8.8	3.4	6.0	8.4	0.1	0.3	0.4	833	1,828	2,665
	NGS	3.7	6.6	9.2	3.5	6.2	8.7	0.2	0.4	0.5	1,143	2,389	3,197

406 SSY: area-specific hillslope sediment yield; SY: hillslope sediment yield. Deposition rates include
 407 hillslope and road deposition. GS: ~~grass buffer strip~~ grass buffer strips; NGS: no ~~grass buffer~~
 408 ~~strip~~ grass buffer strips; Q1: first quartile, or the 25th percentile; Q2: second quartile, or the median;
 409 Q3: third quartile, or the 75th percentile.

410 The comparison between WaTEM/SEDEM simulations and the ~~average annual loads from the~~
 411 ~~monitored tributaries- tributary sediment loads~~ revealed a larger overlap between the latter and the
 412 results from the ‘road-as-shortcuts’ scenario (Figure 7). ~~For this comparison, we only considered the~~
 413 ~~simulations with the presence of grass buffer strips, which more closely represent the actual structure~~
 414 ~~of the agricultural fields in the Baldegg catchment (see Figure 2).~~ The overlap became particularly
 415 clear when we compared the interquartile range (IQR) prediction intervals of the calculations (Figure
 416 7). That is, ~~only a smaller~~ er proportion of the ‘road-as-connectors’ and the ‘road-as-sinks’ model
 417 realisations encompassed the IQR of the tributary sediment loads, except for the Höhibach, which
 418 showed the opposite pattern. This behaviour was particularly evident for the scenario with the
 419 presence of grass buffer strips.



420
 421
 422 Figure 7. Box-plots of hillslope sediment loads simulated by WaTEM/SEDEM for the road
 423 connectivity scenarios for each tributary sub-catchment. Dashed lines represent the median (in black)
 424 and the percentiles-95% interval (in grey) of the measurement-based estimates of sediment loads for

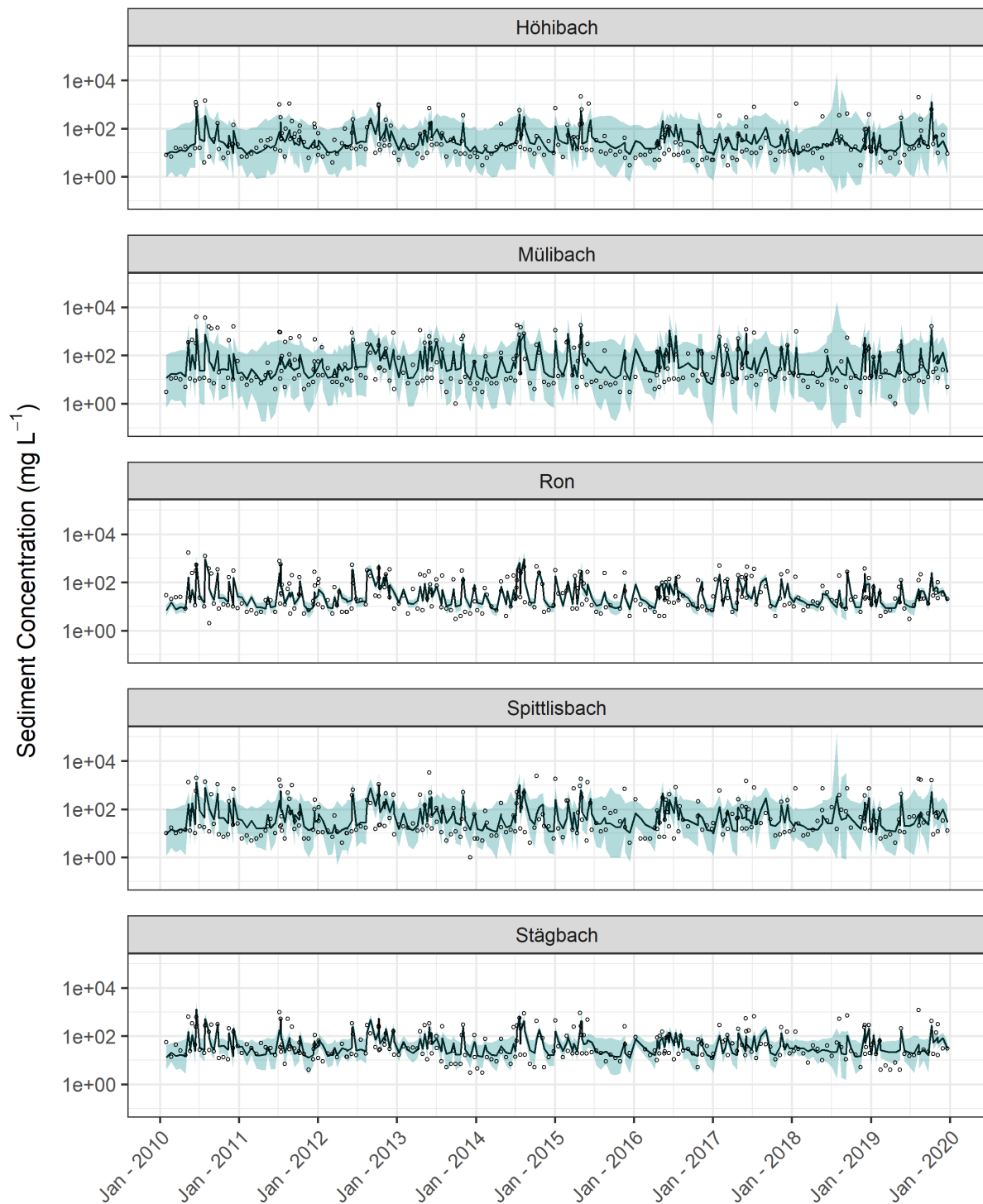
425 each tributary, calculated ~~based on from~~ the error propagation of the sediment-rating curve. GS: grass
 426 buffer strips, NGS: no grass buffer strips. Simulations for the shortcut scenario generally shows a
 427 higher overlap with calculated sediment loads, in particular when grass buffer strips are considered.

428 It is important to note that the median sediment concentrations calculated by the rating curve
 429 (Equation 1) underestimated the actual observations, for all tributaries. This is expressed by the
 430 positive mean error of the estimates (Table 4). Moreover, the Nash-Sutcliffe model efficiency
 431 coefficient for the median calculations was unsatisfactory considering the usual thresholds for model
 432 performance (e.g. Moriasi et al., 2015). On the other hand, the 95 % prediction interval of the rating
 433 curve encompassed a large proportion of the observations, and most errors were associated to extreme
 434 events (Table 4, Figure 8). Hence, it is likely that actual sediment loads from the tributaries are
 435 contained within the long right side of the skewed distributions resulting from the error propagation of
 436 the rating curves (Figure ~~78~~), which would increase the overlap with the shortcut scenario.

437 Table 4. Evaluation metrics of the sediment rating curve, considering the measured sediment
 438 concentrations and median of the simulations.

Stream	ME ----- mg L ⁻¹ -----	RSME	Out of bound percentage* ----- % -----	r _p	r _s	NSE
Höhibach	50.10	80.60	130.13	0.52	0.64	0.22
Mülibach	72.97	138.32	110.11	0.64	0.73	0.34
Ron	22.00	54.61	0.6161	0.63	0.77	0.38
Spittlisbach	95.67	149.78	0.2222	0.51	0.67	0.20
Stägbach	25.05	67.14	0.3636	0.50	0.70	0.19

439 *percentage of observations out of the 95 % prediction interval. ME: mean error; RMSE: root-mean-
 440 square error, r_p: Pearson's correlation coefficient, r_s: Spearman's correlation coefficient; NSE: Nash-
 441 Sutcliffe model efficiency coefficient.



442

443 Figure 8. Log-scaled daily sediment concentrations estimates from the rating curve: dark solid line is
 444 the median of the calculations and the shaded light blue represents the 95 % prediction interval. Open
 445 circles are the observed values used for fitting the curve.

446 **4 Discussion**

447 Here we assessed the interaction between landscape patchiness, linear structures, and sediment
 448 connectivity. Our quantitative model-based approach highlighted the importance of roads in

449 (dis)connecting sediment fluxes between landscape compartments and surface waters in patchy
450 agricultural catchments, ~~which are typical of the Swiss Plateau~~. These findings are ~~very much~~ in lines
451 with long-term field observations and qualitative model assessments for similar areas in Switzerland.

452 For instance, Ledermann et al. (2010) monitored off-site erosion in multiple fields from different
453 regions of the Swiss midlands, and found that linear features in general and roads in particular had a
454 large influence on runoff concentration, soil erosion rates, and off-site damage. These authors also
455 estimated that > 50 % of eroded soil was deposited in adjacent fields and infra-structure, while up to
456 20 % reached surface waters, mainly through indirect inflow via the road and drainage network. Such
457 figures are proportionate to WaTEM/SEDEM estimations for the Baldegg catchment, specifically for
458 the shortcut scenario with the presence of ~~grass-buffer-strip~~ grass buffer strips (Table 3). Another
459 interesting similarity between our outputs and the field assessments from Ledermann et al. (2010), was
460 that both approaches identified field border structures as critical regulators of soil erosion and
461 sediment transport (see Figures 5 and 6). According to the field assessments, border furrows are
462 specifically important for both triggering erosion and promoting diffuse sediment deposition. Such
463 features, combined with long-term tillage erosion, might be responsible creating the topographic
464 pattern displayed in Figure 6d.

465 Moreover, the capacity of roads to connect runoff and sediments from arable land to surface waters in
466 Switzerland was extensively described by Alder et al. (2015) and Schönenberger and Stamm (2021).
467 Both studies used a similar semi-qualitative modelling approach for identifying agricultural fields that
468 were directly or indirectly (i.e. via the road and drainage networks) connected to surface waters. In
469 particular, Schönenberger and Stamm (2021) mapped the location of drainage inlets in multiple small
470 catchments of the Swiss Plateau. Accordingly, these authors identified the road drainage system as the
471 main ~~hydrological shortcut~~ hydraulic shortcut connecting fields to water courses, as most drainage
472 inlets discharge into surface waters (87%), and only a small proportion of them flow into wastewater
473 treatment plants or depositional areas. Hence, the fact that the WaTEM/SEDEM ‘road as shortcuts’
474 scenario displayed a greater agreement with the sediment rating curves for the Baldegg tributaries
475 (Figure 7) is coherent with the current understanding of runoff dynamics in the Swiss Plateau. Of note,
476 the contrasting results for the Höhibach sediment loads (Figure 7), which are much closer to the sink
477 and patch-connector simulations, do not seem to be explained by any physiographical ~~specificity~~
478 characteristic of the sub-catchment (e.g. stream and road density, slope, or land cover). Hence, we
479 speculate that this different pattern could be caused by a lower inlet drainage density or cropping
480 specificities in the Höhibach ~~sub-catchment contributing area, or by in-stream process, that are not~~
481 ~~accounted for in WaTEM/SEDEM.~~

482 In addition, our simulations of edge-of-field ~~grass-buffer-strip~~ grass buffer strips indicated that these
483 structures might be particularly relevant for the ‘road as shortcuts’ scenario. In this case, the model
484 estimated that grass-trips could reduce up to 30% the sediment connectivity from hillslopes to surface

485 waters in the Baldegg catchment (Table 4). However, it should be noted that we assumed 2 m wide
486 strips at field_block borders, irrespectively of the adjacent structures or land use. As previously
487 mentioned, the extent of these features is in fact quite variable, and legislation only requires 0.5 m
488 filters between fields and roads, as reported by Alder et al. (2015). These authors further emphasised
489 that albeit edge-of-field strips are an important complementary management practice, their
490 effectiveness is often reduced [at high inflow in case of large drainage](#) areas, in which very wide buffers
491 would be necessary to stop sediment fluxes. Hence, Alder et al. (2015) recommended that minimising
492 on-site erosion rates was ultimately the most effective way to decrease sediment input from arable land
493 to water courses in Switzerland. Our results support this management proposition. However, our
494 simulations also indicate that the disproportional sediment connectivity afforded by the dense road
495 network translates into an excessive sediment supply to water courses, even when simulated erosion
496 rates were small. As on-site erosion rates in Switzerland are already reasonably low (see Prasuhn,
497 2020), it might be important to consider solutions that address the sediment transport through the
498 underground drainage system, particularly in environmentally sensitive areas, such as the Baldegg
499 catchment.

500 In a wider context, our study has demonstrated how structural sediment connectivity patterns can be
501 investigated with a conceptual model as WaTEM/SEDEM, provided that model resolution is
502 sufficiently fine to represent relevant features and processes. In ~~the Baldegg catchment, and likely in~~
503 ~~other patchy~~ agricultural [landscapes catchments of the Swiss Plateau and likely in other patchy](#)
504 [landscapes](#), soil redistribution rates and patterns are intrinsically linked to linear features (see Alder et
505 al., 2015; Ledermann et al., 2010; Prasuhn, 2020; Remund et al., 2021). Hence, in order to provide
506 relevant system descriptions, soil erosion models applied under similar conditions must be able to
507 represent linear features and landscape patchiness. Although ~~these our~~ results might seem case-
508 specific, similar findings have been reported around the world. For instance, the effects of roads and
509 farm tracks in both coupling and decoupling runoff and sediments has been described in Australia
510 (Croke et al., 2005), Brazil (Bispo et al., 2020), Kenya (Stenfert Kroese et al., 2020), Italy (Persichillo
511 et al., 2018), ~~and~~ Spain (Calsamiglia et al., 2018), [and the USA](#) (Mahoney et al., 2018). Moreover, the
512 influence of linear features such as field borders, hedges, terraces, and tractor tram lines ~~in on~~ soil
513 redistribution ~~rates rates and patterns~~ have been well_documented in Europe (Calsamiglia et al.,
514 2018b; Evrard et al., 2009; Fiener and Auerswald, 2005; Lacoste et al., 2014; Saggau et al., 2019), as
515 well as the importance of landscape structure [in regulating sediment connectivity](#) (Baartman et al.,
516 2020; Chartin et al., 2013; Fiener et al., 2011).

517 Another generalisable finding from our research was that WaTEM/SEDEM can be as sensitive to
518 RUSLE parameters as to the model-specific transport capacity coefficients. Therefore, when
519 performing uncertainty analyses of WaTEM/SEDEM, it is important to consider sources of error
520 associated to the RUSLE parameterisation. So far, uncertainty estimation methods applied to

521 WaTEM/SEDEM have focused on the K_{TC} parameterisation, and therefore have underestimated the
522 uncertainty in model predictions. We anticipate that our open-source WaTEM/SEDEM script will
523 facilitate stochastic implementations of the model, and ultimately promote uncertainty and sensitivity
524 analysis of soil erosion models. In particular, the open-source code will allow model users to explore
525 structural uncertainties, which can contribute to increase our understanding of sediment connectivity
526 processes. As recent studies have again demonstrated, ~~results from soil erosion models are only~~
527 ~~interpretable if the uncertainty in model structures, parameter estimation, and observational forcing~~
528 ~~data are accounted for investigating the uncertainty in model structures, parameter estimation, and~~
529 ~~observational testing data is crucial for advancing soil erosion modelling research~~ (Benaud et al.,
530 2021; Eekhout et al., 2021; Schürz et al., 2020).

531 Importantly, while we demonstrated how conceptual models such as WaTEM/SEDEM can be useful
532 for understanding structural connectivity patterns, more dynamic and process-oriented models are
533 necessary for identifying so-called hot spots and hot moments of sediment connectivity (Owens, 2020;
534 Turnbull and Wainwright, 2019). In addition, WaTEM/SEDEM representations of sediment transfer
535 could be improved by incorporating the (dis)connectivity caused by linear features other than parcel
536 borders and grass buffer strips. This might entail assimilating the P_{Con} parameter to features such as
537 roadside ditches or terraces. Finally, mapping the location of hydraulic shortcuts within the road
538 network, as well as the extent to which these shortcuts increase the connectivity from hillslopes to
539 water courses (e.g., Schönenberger and Stamm, 2021), should further improve sediment connectivity
540 simulations in areas such as the Baldegg catchment.

541 **5 Conclusions**

542 Here we employed a global sensitivity analysis of the WaTEM/SEDEM model to investigate the
543 influence of linear structures and landscape patchiness on sediment connectivity in the Baldegg
544 catchment, ~~a representative area of Swiss Plateau.~~ In particular, this novel application of
545 WaTEM/SEDEM was implemented with the free [programming language R](#), and our code
546 is available as supplementary material.

547 Our results demonstrated that assumptions about road connectivity were by far the most important
548 factor for modelling sediment transfer in the Baldegg catchment. Moreover, the comparison between
549 extensive model simulations and sediment rating₋curve calculations indicated that roads and hydraulic
550 shortcuts are likely to behave as conduits for sediment transport in the catchment. Hence, representing
551 road connectivity is crucial for modelling sediment transfer from hillslope to water courses in this
552 agricultural catchment of the Swiss Plateau, and potentially in other areas with a dense road drainage
553 system. Moreover, our results further highlighted the effects of linear structures and landscape
554 patchiness on sediment connectivity. These findings were made possible by the use of a model that
555 was specifically tailored to explore the particularities of our study area, by effectively exploring model
556 assumptions and the parameter space, and by the use of high₋resolution spatial data.

557 Overall, we found that WaTEM/SEDEM was useful for investigating sediment connectivity in the
558 Baldegg catchment, as it allowed us to unravel some of the processes and structures regulating
559 hillslope sediment transport in the area. ~~If these processes and structures are accounted for, the model~~
560 ~~shows potential for upscaling.~~In the case the model is ~~be~~ used for prediction and decision-making, we
561 recommend employing a fit-for-purpose rejectionist model testing framework, with multiple sources
562 of data, in order to evaluate the model's numerical accuracy and the quality of its spatial predictions.

563 **6 Code availability**

564 The code for the model simulations was uploaded as a supplementary material file. If the manuscript is
565 accepted, we will upload the R script file and input data used for the simulations to the EnviDat
566 platform (<https://www.envidat.ch>).

567 **7 Data availability**

568 If the manuscript is accepted, we will upload the input data used for the simulations, and the raw
569 sediment and discharge data to the EnviDat platform (<https://www.envidat.ch>). ~~This includes:~~

570 ~~Processed DEM~~

571 ~~Edited land cover rasters with the locations of grass buffer strips~~

572 ~~Road network map~~

573 ~~Field block map~~

574 ~~The raw water discharge and sediment concentration data is property of the Department of~~
575 ~~Environment and Energy of Canton Luzern, and can be shared upon their discretion.~~

576 **8 Author contributions**

577 PVGB and PF developed the model code, PVGB performed the simulations and analysed the data. SS
578 prepared model input data. PVGB prepared the manuscript with contributions from all authors. CA
579 was part of discussing ideas and revised the manuscript. ~~CA revised the manuscript.~~

580 **9 Competing interests**

581 The authors declare no conflict of interest.

582 **10 Acknowledgements**

583 The authors would like to thank Robert Lovas, from the department of environment and energy of the
584 Canton Luzern of Lucerne, who supplied for supplying the sediment concentration and water discharge
585 monitoring data used in this manuscript, and commenting on an earlier draft of this manuscript. We
586 also appreciate the help from Axel Birkholz in acquiring the data. PVGB would like to thank Franz

587 Conen and Claudia Mignani for their multiple and valuable inputs regarding the conceptualisation and
588 preparation of this manuscript.

589

590 **References**

- 591 Alder, S., Prasuhn, V., Liniger, H., Herweg, K., Hurni, H., Candinas, A. and Gujer, H. U.: A high-
592 resolution map of direct and indirect connectivity of erosion risk areas to surface waters in
593 Switzerland-A risk assessment tool for planning and policy-making, *Land use policy*, 48, 236–249,
594 doi:10.1016/j.landusepol.2015.06.001, 2015.
- 595 Antoniadis, A., Lambert-Lacroix, S. and Poggi, J. M.: Random forests for global sensitivity analysis:
596 A selective review, *Reliab. Eng. Syst. Saf.*, 206, 107312, doi:10.1016/j.ress.2020.107312, 2021.
- 597 von Arb, C., Stoll, S., Frossard, E., Stamm, C. and Prasuhn, V.: The time it takes to reduce soil legacy
598 phosphorus to a tolerable level for surface waters: What we learn from a case study in the catchment
599 of Lake Baldegg, Switzerland, *Geoderma*, 403, doi:10.1016/j.geoderma.2021.115257, 2021.
- 600 Baartman, J. E. M., Nunes, J. P., Masselink, R., Darboux, F., Biielders, C., Degré, A., Cantreul, V.,
601 Cerdan, O., Grangeon, T., Fiener, P., Wilken, F., Schindewolf, M. and Wainwright, J.: What do
602 models tell us about water and sediment connectivity?, *Geomorphology*, 367, 107300,
603 doi:10.1016/j.geomorph.2020.107300, 2020.
- 604 BAFU: Faktenblatt: Der Greifensee, Zustand bezüglich Wasserqualität, 1–8 [online] Available from:
605 <http://www.bafu.admin.ch>, 2016.
- 606 Bakker, M. M., Govers, G., van Doorn, A., Quetier, F., Chouvardas, D. and Rounsevell, M.: The
607 response of soil erosion and sediment export to land-use change in four areas of Europe: The
608 importance of landscape pattern, *Geomorphology*, 98(3–4), 213–226,
609 doi:10.1016/j.geomorph.2006.12.027, 2008.
- 610 Batista, P. V. G., Laceby, J. P., Davies, J., Carvalho, T. S., Tassinari, D., Silva, M. L. N., Curi, N. and
611 Quinton, J. N.: A framework for testing large-scale distributed soil erosion and sediment delivery
612 models : Dealing with uncertainty in models and the observational data, *Environ. Model. Softw.*, 137,
613 doi:10.1016/j.envsoft.2021.104961, 2021.
- 614 Bauer, M., Dostal, T., Krasa, J., Jachymova, B., David, V., Devaty, J., Strouhal, L. and Rosendorf, P.:
615 Risk to residents, infrastructure, and water bodies from flash floods and sediment transport, *Environ.*
616 *Monit. Assess.*, 191(2), doi:10.1007/s10661-019-7216-7, 2019.
- 617 Benaud, P., Anderson, K., Evans, M., Farrow, L., Glendell, M., James, M. R., Quine, T. A., Quinton,
618 J. N., Rickson, R. J. and Brazier, R. E.: Reproducibility, open science and progression in soil erosion
619 research. A reply to “Response to ‘National-scale geodata describe widespread accelerated soil
620 erosion’ Benaud et al. (2020) *Geoderma* 271, 114378” by Evans and Boardman (2021), *Geoderma*,
621 402, doi:10.1016/j.geoderma.2021.115181, 2021.

622 Bircher, P., Liniger, H. and Prasuhn, V.: Aktualisierung und Optimierung der Erosionsrisikokarte (
623 ERK2) Die neue ERK2 (2019) für das Ackerland der Schweiz, 2019.

624 Bispo, D. F. A., Batista, P.V.G., Guimarães, D. V., Silva, M. L. N., Curi, N. and Quinton, J. N.:
625 Monitoring land use impacts on sediment production : a case study of the pilot catchment from the
626 Brazilian program of payment for environmental services, *Rev. Bras. Ciência do Solo*, 44, :e0190167,
627 2020.

628 Boardman, J.: A 38-year record of muddy flooding at Breaky Bottom: Learning from a detailed case
629 study, *Catena*, 189(January), 104493, doi:10.1016/j.catena.2020.104493, 2020.

630 Borselli, L., Cassi, P. and Torri, D.: Prolegomena to sediment and flow connectivity in the landscape:
631 A GIS and field numerical assessment, *Catena*, 75(3), 268–277, doi:10.1016/j.catena.2008.07.006,
632 2008.

633 Breiman, L.: Random forests, *Machine Learning*, 45, 5-32, 2001.

634 Brenning, A., Bangs, D., Becker, M.: RSAGA: SAGA geoprocessing and terrain analysis. R package
635 version 1.3.0., 2018.

636 Calsamiglia, A., García-Comendador, J., Fortesa, J., López-Tarazón, J. A., Crema, S., Cavalli, M.,
637 Calvo-Cases, A. and Estrany, J.: Effects of agricultural drainage systems on sediment connectivity in a
638 small Mediterranean lowland catchment, *Geomorphology*, 318, 162–171,
639 doi:10.1016/j.geomorph.2018.06.011, 2018a.

640 Calsamiglia, A., Fortesa, J., García-Comendador, J., Lucas-Borja, M. E., Calvo-Cases, A. and Estrany,
641 J.: Spatial patterns of sediment connectivity in terraced lands: Anthropogenic controls of catchment
642 sensitivity, *L. Degrad. Dev.*, 29(4), 1198–1210, doi:10.1002/ldr.2840, 2018b.

643 Cavalli, M., Trevisani, S., Comiti, F. and Marchi, L.: Geomorphometric assessment of spatial
644 sediment connectivity in small Alpine catchments, *Geomorphology*, 188, 31–41,
645 doi:10.1016/j.geomorph.2012.05.007, 2013.

646 Chartin, C., Evrard, O., Salvador-Blanes, S., Hirschberger, F., Van Oost, K., Lefèvre, I., Daroussin, J.
647 and Macaire, J. J.: Quantifying and modelling the impact of land consolidation and field borders on
648 soil redistribution in agricultural landscapes (1954-2009), *Catena*, 110, 184–195,
649 doi:10.1016/j.catena.2013.06.006, 2013.

650 Conrad, O., Bechtel, B., Bock, M., Dietrich, H., Fischer, E., Gerlitz, L., Wehberg, J., Wichmann, V.
651 and Böhner, J.: System for Automated Geoscientific Analyses (SAGA) v.2.2.2, 1991–2007,
652 doi:10.5194/gmd-8-1991-2015, 2015.

653 Croke, J., Mockler, S., Fogarty, P. and Takken, I.: Sediment concentration changes in runoff pathways
654 from a forest road network and the resultant spatial pattern of catchment connectivity,
655 *Geomorphology*, 68(3–4), 257–268, doi:10.1016/j.geomorph.2004.11.020, 2005.

656 Desmet, P., Govers, G.: A GIS procedure for automatically calculating the USLE LS factor on
657 topographically complex landscape units, *J. Soil Water Conserv.*, 51, 427–433, 1996.

658 Eekhout, J. P. C., Millares-Valenzuela, A., Martínez-Salvador, A., García-Lorenzo, R., Pérez-Cutillas,
659 P., Conesa-García, C. and de Vente, J.: A process-based soil erosion model ensemble to assess model
660 uncertainty in climate-change impact assessments, *L. Degrad. Dev.*, 32, 2409–2422,
661 doi:10.1002/ldr.3920, 2021.

662 Evrard, O., Cerdan, O., van Wesemael, B., Chauvet, M., Le Bissonnais, Y., Raclot, D., Vandaele, K.,
663 Andrieux, P. and Bielders, C.: Reliability of an expert-based runoff and erosion model: Application of
664 STREAM to different environments, *Catena*, 78(2), 129–141, doi:10.1016/j.catena.2009.03.009, 2009.

665 Fiener, P. and Auerswald, K.: Measurement and modeling of concentrated runoff in grassed
666 waterways, *J. Hydrol.*, 301(1–4), 198–215, doi:10.1016/j.jhydrol.2004.06.030, 2005.

667 Fiener, P., Auerswald, K. and Van Oost, K.: Spatio-temporal patterns in land use and management
668 affecting surface runoff response of agricultural catchments-A review, *Earth-Science Rev.*, 106(1–2),
669 92–104, doi:10.1016/j.earscirev.2011.01.004, 2011.

670 Fiener, P., Wilken, F. and Auerswald, K.: Filling the gap between plot and landscape scale – eight
671 years of soil erosion monitoring in 14 adjacent watersheds under soil conservation at Scheyern,
672 Southern Germany, *Adv. Geosci. Discuss.*, (July), doi:adgeo-2019-4, 2019.

673 Fryirs, K.: (Dis)Connectivity in catchment sediment cascades: A fresh look at the sediment delivery
674 problem, *Earth Surf. Process. Landforms*, 38(1), 30–46, doi:10.1002/esp.3242, 2013.

675 Gelman, A. and Hill, J.: *Data Analysis Using Regression and Multilevel/Hierarchical Models*,
676 Cambridge University Press, New York., 2007.

677 Govers, G.: Misapplications and misconceptions of erosion models, in: *Handbook of erosion*
678 *modelling*, edited by: Morgan, R. P. C., Nearing, M.A., Blackwell Publishing Ltd., Chichester, United
679 Kingdom, 117–134, 2011.

680 Heckmann, T., Cavalli, M., Cerdan, O., Foerster, S., Javaux, M., Lode, E., Smetanová, A., Vericat, D.
681 and Brardinoni, F.: Indices of sediment connectivity: opportunities, challenges and limitations, *Earth-*
682 *Science Rev.*, 187(December 2017), 77–108, doi:10.1016/j.earscirev.2018.08.004, 2018.

683 [IUSS Working Group WRB. World Reference Base for Soil Resources; IUSS Working Group WRB:](#)
684 [Wageningen, The Netherlands, 2006; pp. 1–128.](#)

685 Keller, B.: Lake Lucerne and its spectacular landscape, in: Landscapes and landforms of Switzerland,
686 edited by Reynard, E., Springer Nature Switzerland, Cham, Switzerland, 305-324, 2021.

687 Krasa, J., Dostal, T., Jachymova, B., Bauer, M. and Devaty, J.: Soil erosion as a source of sediment
688 and phosphorus in rivers and reservoirs – Watershed analyses using WaTEM/SEDEM, *Environ. Res.*,
689 171(January), 470–483, doi:10.1016/j.envres.2019.01.044, 2019.

690 Kupferschmied, P.: CP-Tool: Ein Programm zur Berechnung des Fruchtfolge- und
691 Bewirtschaftungsfaktors (CP-Faktor) der Allgemeinen Bodenabtragungsgleichung (ABAG), 2019.

692 Laceby, J. P., Batista, P. V. G., Taube, N., Kruk, M. K., Chung, C., Evrard, O. and Orwin, J. F.:
693 Tracing total and dissolved material in a western Canadian basin using quality control samples to
694 guide the selection of fingerprinting parameters for modelling, *Catena*, 200(April 2020), 105095,
695 doi:10.1016/j.catena.2020.105095, 2021.

696 Lacoste, M., Michot, D., Viaud, V., Evrard, O. and Walter, C.: Combining ^{137}Cs measurements and a
697 spatially distributed erosion model to assess soil redistribution in a hedgerow landscape in
698 northwestern France (1960-2010), *Catena*, 119, 78–89, doi:10.1016/j.catena.2014.03.004, 2014.

699 Lavrieux, M., Birkholz, A., Meusburger, K., Wiesenberg, G. L. B., Gilli, A., Stamm, C. and Alewell,
700 C.: Plants or bacteria? 130 years of mixed imprints in Lake Baldegg sediments (Switzerland), as
701 revealed by compound-specific isotope analysis (CSIA) and biomarker analysis, *Biogeosciences*,
702 16(10), 2131–2146, doi:10.5194/bg-16-2131-2019, 2019.

703 Ledermann, T., Herweg, K., Liniger, H. P., Schneider, F., Hurni, H. and Prasuhn, V.: Applying
704 erosion damage mapping to assess and quantify off-site effects of soil erosion in Switzerland, *L.*
705 *Degrad. Dev.*, 21, 353–366, 2010.

706 Liaw, A., Wiener, M.: Classification and regression by randomForest. *R News*, 2, 18–22, 2002.

707 Mahoney, D. T., Fox, J. F. and Al-Aamery, N.: Watershed erosion modeling using the probability of
708 sediment connectivity in a gently rolling system, *J. Hydrol.*, 561(April), 862–883,
709 doi:10.1016/j.jhydrol.2018.04.034, 2018.

710 Mahoney, D. T., Fox, J., Al-Aamery, N. and Clare, E.: Integrating connectivity theory within
711 watershed modelling part I: Model formulation and investigating the timing of sediment connectivity,
712 *Sci. Total Environ.*, 740, 140385, doi:10.1016/j.scitotenv.2020.140385, 2020a.

713 Mahoney, D. T., Fox, J., Al-Aamery, N. and Clare, E.: Integrating connectivity theory within
714 watershed modelling part II: Application and evaluating structural and functional connectivity, *Sci.*
715 *Total Environ.*, 740, 140386, doi:10.1016/j.scitotenv.2020.140386, 2020b.

716 MeteoSwiss. SwissMetNet Surface Weather Stations, Mosen MOA, 2010-2019 (Switzerland), 2021.

717 Müller, B., Gächter, R. and Wüest, A.: Accelerated water quality improvement during
718 oligotrophication in peri-alpine lakes, *Environ. Sci. Technol.*, 48(12), 6671–6677,
719 doi:10.1021/es4040304, 2014.

720 Notebaert, B., Vaes, B., Govers, G., Van Oost, K., Van Rompaey, A., and Verstraeten, G.: *WaTEM /*
721 *SEDEM version 2006 Manual.*, 2006.

722 Nunes, J. P., Wainwright, J., Biielders, C. L., Darboux, F., Fiener, P., Finger, D. and Turnbull, L.:
723 Better models are more effectively connected models, *Earth Surf. Process. Landforms*, 43(6), 1355–
724 1360, doi:10.1002/esp.4323, 2018.

725 Owens, P. N.: Soil erosion and sediment dynamics in the Anthropocene: a review of human impacts
726 during a period of rapid global environmental change, *J. Soils Sediments*, 20(12), 4115–4143,
727 doi:10.1007/s11368-020-02815-9, 2020.

728 Parsons, A. J., Wainwright, J., Brazier, R. E. and Powell, D. M.: Is sediment delivery a fallacy? Reply,
729 *Earth Surf. Process. Landforms*, 34(February), 155–161, doi:10.1002/esp, 2009.

730 Persichillo, M. G., Bordoni, M., Cavalli, M., Crema, S. and Meisina, C.: The role of human activities
731 on sediment connectivity of shallow landslides, *Catena*, 160(August 2016), 261–274,
732 doi:10.1016/j.catena.2017.09.025, 2018.

733 Pianosi, F., Beven, K., Freer, J., Hall, J. W., Rougier, J., Stephenson, D. B. and Wagener, T.:
734 Sensitivity analysis of environmental models: A systematic review with practical workflow, *Environ.*
735 *Model. Softw.*, 79, 214–232, doi:10.1016/j.envsoft.2016.02.008, 2016.

736 Pfiffner, O. A.: The structural landscapes of Central Switzerland, in: *Landscapes and landforms of*
737 *Switzerland*, edited by Reynard, E., Springer Nature Switzerland, Cham, Switzerland, 159-172, 2021.

738 Prasuhn, V.: Twenty years of soil erosion on-farm measurement: annual variation, spatial distribution
739 and the impact of conservation programmes for soil loss rates in Switzerland, *Earth Surf. Process.*
740 *Landforms*, doi:10.1002/esp.4829, 2020.

741 Remund, D., Liebisch, F., Liniger, H. P., Heinimann, A. and Prasuhn, V.: The origin of sediment and
742 particulate phosphorus inputs into water bodies in the Swiss Midlands – A twenty-year field study of
743 soil erosion, *Catena*, 203(March), 105290, doi:10.1016/j.catena.2021.105290, 2021.

744 Renard, K., Foster, G. R., Weesies, G. A., McCool, D. K. and Yoder, D. C.: *Predicting Soil Erosion by*
745 *Water: A Guide to Conservation Planning With the Revised Universal Soil Loss Equation (RUSLE)*,
746 1997.

747 R Core Team. *R: A language for statistical computing.* R Foundation for Statistical Computing,
748 Vienna, Austria. URL <https://www.R-project.org>, 2021.

749 Saggau, P., Kuhwald, M. and Duttmann, R.: Integrating soil compaction impacts of tramlines into soil
750 erosion modelling: A field-scale approach, *Soil Syst.*, 3(3), 1–28, doi:10.3390/soilsystems3030051,
751 2019.

752 Schmidt, S., Alewell, C., Panagos, P. and Meusburger, K.: Regionalization of monthly rainfall
753 erosivity patterns in Switzerland, *Hydrol. Earth Syst. Sci.*, 20(10), 4359–4373, doi:10.5194/hess-20-
754 4359-2016, 2016.

755 Schmidt, S., Ballabio, C., Alewell, C., Panagos, P. and Meusburger, K.: Filling the European blank
756 spot—Swiss soil erodibility assessment with topsoil samples, *J. Plant Nutr. Soil Sci.*, 181(5), 737–748,
757 doi:10.1002/jpln.201800128, 2018a.

758 Schmidt, S., Alewell, C. and Meusburger, K.: Mapping spatio-temporal dynamics of the cover and
759 management factor (C-factor) for grasslands in Switzerland, *Remote Sens. Environ.*, 211(April), 89–
760 104, doi:10.1016/j.rse.2018.04.008, 2018b.

761 Schönenberger, U. and Stamm, C.: Hydraulic shortcuts increase the connectivity of arable land areas
762 to surface waters, *Hydrol. Earth Syst. Sci.*, 25(4), 1727–1746, doi:10.5194/hess-25-1727-2021, 2021.

763 Schürz, C., Mehdi, B., Kiesel, J., Schulz, K. and Herrnegger, M.: A systematic assessment of
764 uncertainties in large-scale soil loss estimation from different representations of USLE input factors—a
765 case study for Kenya and Uganda, *Hydrol. Earth Syst. Sci.*, 24(9), 4463–4489, doi:10.5194/hess-24-
766 4463-2020, 2020.

767 Starkloff, T. and Stolte, J.: Applied comparison of the erosion risk models EROSION 3D and LISEM
768 for a small catchment in Norway, *Catena*, 118, 154–167, doi:10.1016/j.catena.2014.02.004, 2014.

769 Stenfert Kroese, J., Batista, P. V. G., Jacobs, S. R., Breuer, L., Quinton, J. N. and Rufino, M. C.:
770 Agricultural land is the main source of stream sediments after conversion of an African montane
771 forest, *Sci. Rep.*, 10(1), 1–15, doi:10.1038/s41598-020-71924-9, 2020.

772 Stoll, S., Arb, C. von, Jorg, C., Kopp, S. and Prasuhn, V.: Evaluation der stark zur Phosphor-Belastung
773 des Baldeggersees beitragenden Flächen., 2019.

774 Swisstopo. SwissALTI3D. Das hoch aufgelöste Terrainmodell der Schweiz, 2014a.

775 Swisstopo. Swissimage. Das digitale Farbornthophotomosaik der Schweiz. 2014b.

776 Swisstopo. SwissTLM3D. Das grossmassstäbliche Topografische Landschaftsmodell der Schweiz,
777 2020.

778 Teranes, J. L. and Bernasconi, S. M.: Factors controlling $\delta^{13}\text{C}$ values of sedimentary carbon in
779 hypertrophic Baldeggersee, Switzerland, and implications for interpreting isotope excursions in lake
780 sedimentary records, *Limnol. Oceanogr.*, 50(3), 914–922, doi:10.4319/lo.2005.50.3.0914, 2005.

781 Turnbull, L. and Wainwright, J.: From structure to function: Understanding shrub encroachment in
782 drylands using hydrological and sediment connectivity, *Ecol. Indic.*, 98(November 2018), 608–618,
783 doi:10.1016/j.ecolind.2018.11.039, 2019.

784 Van Oost, K., Govers, G. and Desmet, P. J. J.: Evaluating the effects of changes in landscape structure
785 on soil erosion by water and tillage, *Landsc. Ecol.*, 15(6), 577–589, doi:10.1023/A:1008198215674,
786 2000.

787 Van Rompaey, A., Verstraeten, G., Van Oost, K., Govers, G. and Poesen, J.: Modelling mean annual
788 sediment yield using a distributed approach, *Earth Surf. Process. Landforms*, 26(11), 1221–1236,
789 doi:10.1002/esp.275, 2001.

790 Verstraeten, G., Van Oost, K., Van Rompaey, A. J. J., Poesen, J. and Govers, G.: Evaluating an
791 integrated approach to catchment management to reduce soil loss and sediment pollution through
792 modelling, *Soil Use Manag.*, 18(4), 386–394, doi:10.1111/j.1475-2743.2002.tb00257.x, 2010.

793 Vigiak, O. and Bende-Michl, U.: Estimating bootstrap and Bayesian prediction intervals for
794 constituent load rating curves, *Water Resour. Res.*, 49(12), 8565–8578, doi:10.1002/2013WR013559,
795 2013.

796 Wainwright, J., Turnbull, L., Ibrahim, T. G., Lexartza-Artza, I., Thornton, S. F. and Brazier, R. E.:
797 Linking environmental regimes, space and time: Interpretations of structural and functional
798 connectivity, *Geomorphology*, 126(3–4), 387–404, doi:10.1016/j.geomorph.2010.07.027, 2011.

799 Wang, Y. G., Kuhnert, P. and Henderson, B.: Load estimation with uncertainties from opportunistic
800 sampling data - A semiparametric approach, *J. Hydrol.*, 396(1–2), 148–157,
801 doi:10.1016/j.jhydrol.2010.11.003, 2011.

802 Wehrli, B., Lotter, A. F., Schaller, T. and Sturm, M.: High-resolution varve studies in Baldeggersee
803 (Switzerland): Project overview and limnological background data, *Aquat. Sci.*, 59(4), 285–294,
804 doi:10.1007/BF02522359, 1997.

805 Wilken, F., Fiener, P. and Van Oost, K.: Modelling a century of soil redistribution processes and
806 carbon delivery from small watersheds using a multi-class sediment transport model, *Earth Surf. Dyn.*,
807 5, 113–124, doi:10.5194/esurf-5-113-2017, 2017.

808